Bidirectional Converter Controllers for DC Machines in a Micro Grid Network

G. Sridhar Babu[1], A. Mano Ranjith Kumar[2] , T. Penchalaiah[3], S. Vijay[4]

[1-4]*EEE Department,* [1&3]*St. Martin's Engineering College, Dhulapally,* [2]*Global College of Engineering, Chennur,* [4]*Bharath Institute of Engineering & Technology, Ibrahimptnam*

[1]sridharbabueee@smec.ac.in, [2]manoranjith015@gmil.com, [3]smec.penchal99@gmail.com, [4]svijay0416@gmail.com

***Abstract*— When DC distribution is applied in a system with DC preferred appliances, it is possible to enhance energy consumption efficiency by reducing conversion losses. Moreover, renewable energy sources and storage devices can be fully utilized because they are more compatible with DC based system where generated energy can be directly used to loads and stored which results in less conversion loss. In dc-micro grid applications, a power distribution system requires a bi-directional inverter to control the power flow between dc bus and ac grid, and to regulate the dc bus to a certain range of voltages, in which dc load may change abruptly. Using the analysis of the rectifier's operating modes each switching device can be selected by considering switch stresses. A simple and intuitive frequency detection method for a single-phase synchronous reference frame-phase-locked loop (SRF-PLL) is also proposed using a filter compensator, a fast period detector, and a finite impulse response filter to improve the robustness and accuracy of PLL performance under fundamental frequency variations.**

***Keywords*— AC–DC boost rectifier, bidirectional isolated converter, CLLC resonant converter dc distribution system**

I. INTRODUCTION

The single-phase non isolated bidirectional rectifier typically consists of a conventional full-bridge structure. It has two sinusoidal pulse width modulation (SPWM) methods such as the bipolar and the unipolar switching modes. One of the disadvantages of the bipolar switching mode is the need of a large inductor to reduce the input current ripple because the peak to-peak voltage of the inductor is more than twice the unipolar switching mode. If the full-bridge rectifier operates in the unipolar switching mode, inductance for a continuous current mode (CCM) power factor correction (PFC) operation can be reduced. One of full-bridge rectifier legs in the unipolar switching mode is operated at a line frequency while the other one is modulated at a switching frequency. However, the unipolar switching mode rectifier using conventional switching devices including a normal antiparallel diode causes high reverse recovery current and turn-on switching noise. The switching and the conduction losses in the bidirectional rectifier are the main cause of decreasing power conversion efficiency. The phase estimation, so-called phase-locked loop (PLL), is required to control the bidirectional ac–dc rectifier; especially, the phase information of supply voltage is mandatory to generate a current reference. One of the popular PLL methods is synchronous reference frame (SRF-PLL) which uses a rotating reference frame for tracking a phase angle. However, the conventional SRFPLL has a weak point of frequency tracking performance because it uses the constant angular frequency of a fundamental component. It can cause a tracking error in the PLL operation when the fundamental frequency changes to the different value of the constant angular frequency. Numerous methods for improved PLL have been presented and introduced in the literature. Even though they have good performance against the frequency distortion, their algorithms are complicated to be implemented for various applications.

II. CIRCUIT CONFIGURATION OF THE PROPOSED ISOLATED BIDIRECTIONAL AC–DC CONVERTER

Fig 1 shows the circuit configuration of the proposed isolated bidirectional ac–dc converter. It consists of the single phase bidirectional rectifier for grid interface and the isolated bidirectional full-bridge CLLC resonant converter for galvanic isolation. To control the proposed converter, a single digital signal processor (DSP) controller (TMS320F28335) was used. The power flow directions in the converter are defined as follows: rectification mode (forward direction of power flow) and generation mode (backward direction of power flow). The switching method of the proposed single-phase bidirectional rectifier is unipolar SPWM. In order to reduce the switching losses caused by the reverse recovery current in the rectification mode, the high-side switches of the proposed rectifier are composed of two IGBTs without anti parallel diodes (S1 and S3) and two SiC diodes (DS1 and DS3). The low side switches are composed of two MOSFETs (S2 and S4) for reducing conduction loss and for using ZVS operation in the generation mode. The detailed circuit operation of the proposed bidirectional rectifier and advanced PLL method will be discussed. The proposed bidirectional full-bridge CLLC resonant converter has the full-bridge symmetric structure of the primary inverting stage and secondary rectifying stage with a symmetric transformer. Using the high-frequency transformer, the converter can achieve galvanic isolation between the primary side and the secondary side. The transformer Tr is modelled with the magnetizing inductance Lm and the transformer's turn ratio of 1:1. The leakage inductance of the transformer's primary and secondary windings is merged to the resonant inductor Lr1 and Lr2, respectively.

III. NON ISOLATED AC–DC BIDIRECTIONAL RECTIFIER

High-power rectifiers do not have a wide choice of switching devices because there are not many kinds of the switching devices for high-power capacity. Generally, the full-bridge rectifier in high-power applications consists of the same four devices: IGBT modules or intelligent power modules (IPMs) are chiefly used. These modular devices have anti parallel diodes, which have fast recovery characteristics. A fast recovery diode (FRD) has a small reverse recovery time trr. When the full bridge rectifier operates, the time trr causes a reverse recovery current which increases power loss and EMC problems. Therefore, soft-switching techniques using additional passive or active snubber circuits have been proposed. Even though these methods require a relatively large number of passive or active components, which decrease the reliability of the rectifier system and increase system cost, the soft-switching techniques in the high-power rectifier are a unique solution for reducing the reverse recovery problems. In the bidirectional rectifier using the unipolar switching method, the turn-on period of low-side switches increases one and half times more than the turn on period of the high-side switches. Therefore, the low side IGBTs in the view point of the conduction loss when the same current flows into the switching devices. Therefore, MOSFETs are suitable for the low-side switches in the unipolar switching method.

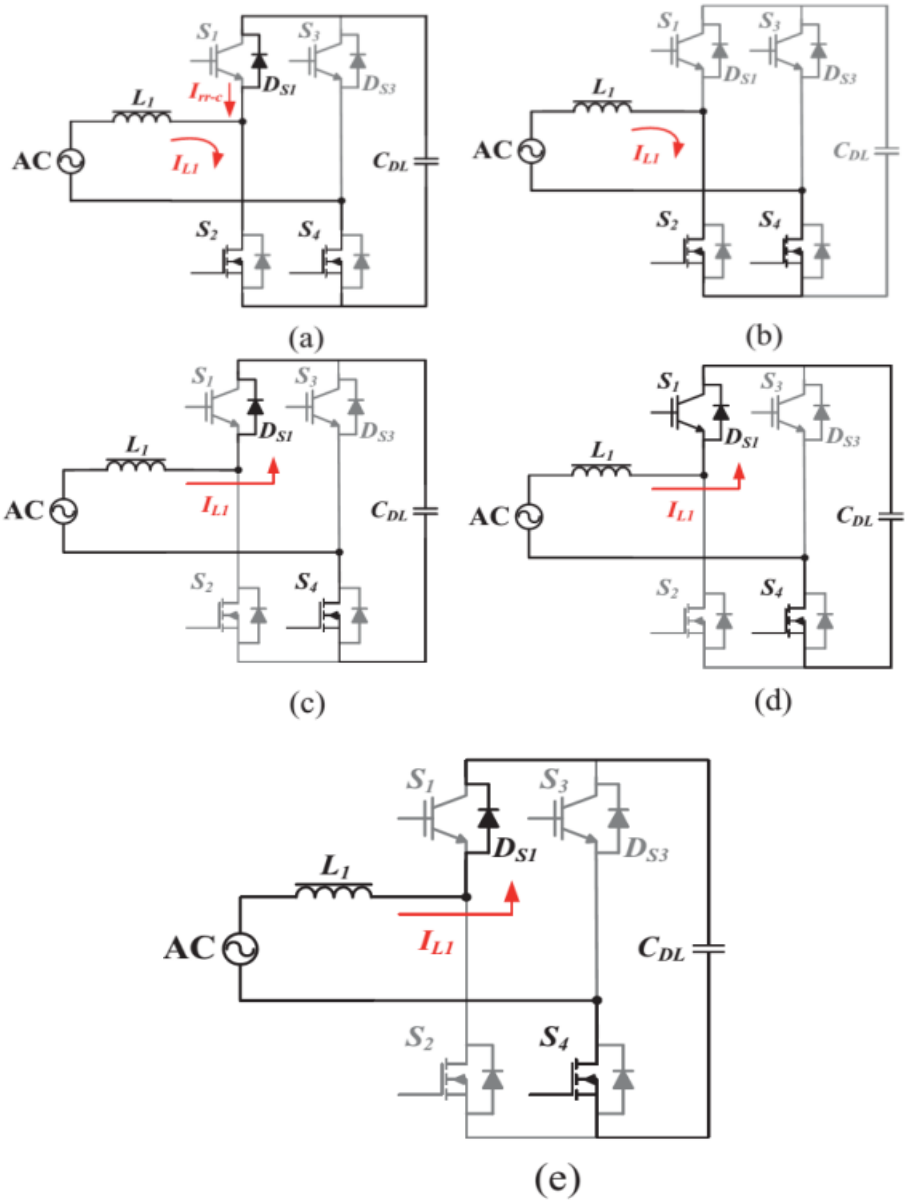

Fig 1 Operating modes of the proposed bidirectional ac–dc rectifier in the rectification mode: (a) Mode1, (b) Mode2, (c) Mode3, (d) Mode4, and (e) Mode5.

A. CONSIDERATION FOR REVERSE ECOVERY LOSSES IN A RECTIFICATION MODE

In the rectification mode, the bidirectional rectifier has five operating modes in a single switching cycle. The circuit operations in the positive half period of the input voltage are shown in Fig 1. The dark lines denote conducting paths for each state. The theoretical waveforms of the proposed rectifier are given in Fig 2 At time t0, the low-side switch S2 turns ON. At this time, if DS1 is FRD, DS1 cannot immediately turn OFF because of its reverse recovery process. Low side switches should be chosen to consider low conduction losses for increasing the power conversion efficiency. The latest generation of MOSFETs employing super junction technology can achieve extremely low on resistance R_{DS}.on. It is better than the latest very low VCE

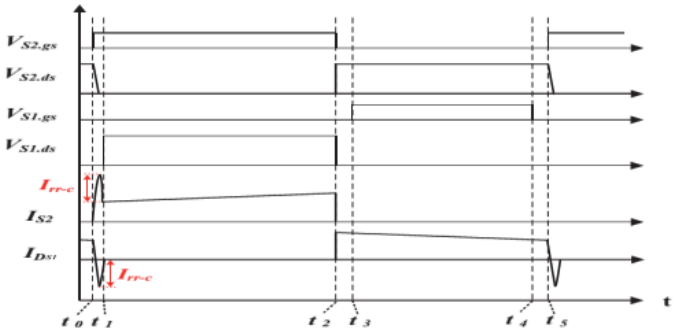

Fig 2 Theoretical operating waveforms of the proposed bidirectional ac–dc

This simultaneous high reverse recovery current causes an additional switching loss on S2. The reverse recovery current increases the current stress on the low side switches and decreases the EMI performance of the rectifier. To solve this reverse recovery problem, the high-side switches of the proposed circuit should use IGBTs without anti parallel diodes and SiC diodes as anti parallel diodes of the IGBTs. Even though the reverse recovery current is not completely zero in a Rectifier in the rectification mode. Practical manner, it is significantly reduced as compared with the FRD operation. At t3, the gate signals VS1.gsturns ON. Since the IGBTs cannot conduct in the reverse direction, the energy in the input voltage source and the inductor L1 is still discharged through SiC diode DS1. In the rectification mode, the high-side SiC diodes instead of the IGBTs are fully operated during entire rectification modes. Therefore, the conduction loss of the high-side switches depends on the forward voltage drop of the SiC diodes. Other operation modes are not different from the conventional full bridge rectifier using a unipolar switching method.

B. CONSIDERATION FOR SWITCHING LOSSES IN A GENERATION MODE

In the generation mode using the same switching pattern as the rectification mode, the proposed bidirectional rectifier has five operating modes in a single switching cycle. The circuit operations in the positive half period of the input voltage are shown in Fig 3 After the discharge operation of dc-link's energy, the anti parallel diode including the low-side switch S2 will be conducted by freewheeling operation using inductor's energy as shown in Mode2. During this period, the energy stored in the output capacitance of S2 can be fully discharged. In Mode 3, S2 turns ON under the ZVS condition. Through these operation modes, the turn-on losses in the low-side switches can be reduced. When the high side switch S1 turns ON in Mode 5, the antiparallel diode of S2 cannot immediately turn OFF because of poor reverse recovery performance of the MOSFET's anti parallel diode. It causes an additional switching loss on S1 through the reverse recovery current. Therefore, the generation mode using the same switching pattern of the rectification mode has advantages of soft switching and disadvantages of reverse recovery loss. The MOSFET's losses in the generation mode depend on the MOSFET's $R_{DS\cdot on}$ and the reverse recovery characteristics of the antiparallel diode. The selection of the MOSFET can determine the significant loss factor between switching and conduction losses.

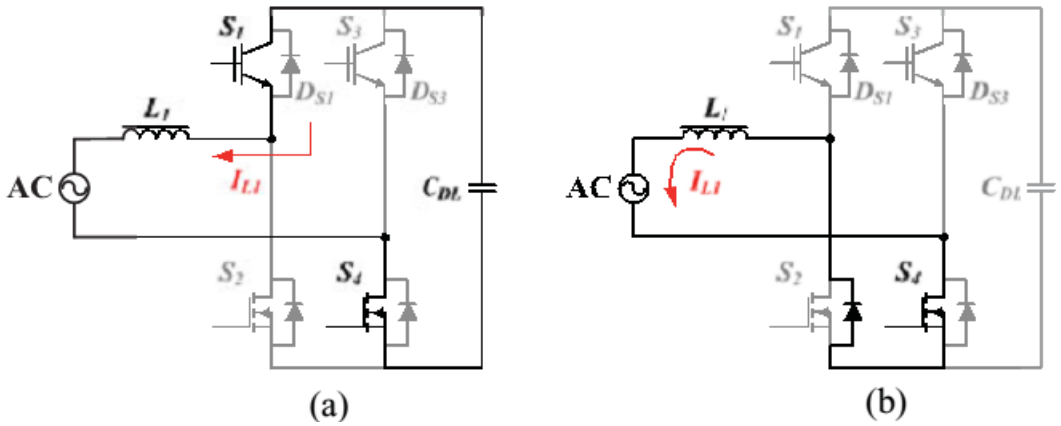

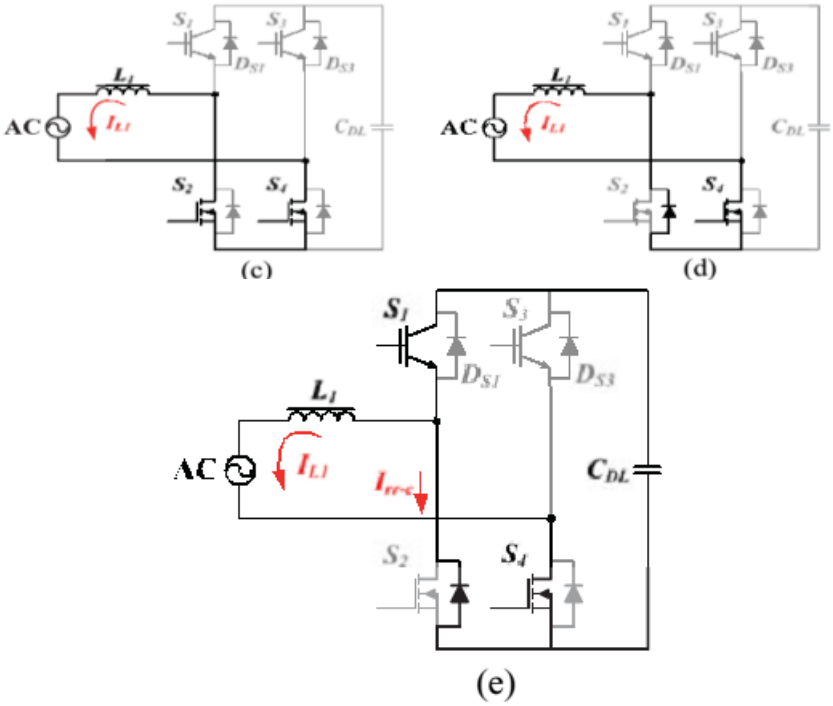

Fig 3 Operating modes in the rectifier's generation mode using the same switching pattern as the rectification mode: (a) Mode1, (b) Mode2, (c) Mode3, (d) Mode4, and (e) Mode5.

However, if IGBTs are used for the low-side switches, the ZVS operation is not significant to reduce their switching loss. There are also reverse recovery losses through the reverse recovery characteristics of the antiparallel diode. They can increase the turn-off switching losses through the IGBT's tailing current. If the reverse recovery loss through the MOSFETs is significant, it can be overcome employing the inverted switching pattern in the generation mode. The operation mode of the inverted switching pattern is shown in Fig 4 In this operation, the switching pattern is perfectly inverted and the turn-on period of the high-side switches is one and half times longer than the turn-on period of the low-side switches. In Mode 5, the low-side switch S4 turns ON. At the same time, the reverse recovery current should be limited by the SiC diode DS3. Using this switching pattern in the generation mode, there are no benefits of the ZVS operation. However, the reverse recovery losses can be significantly reduced as compared with the same switching pattern of the rectification mode. The modified switching pattern does not affect the power conversion and control performances of the ac–dc rectifier.

C. CONSIDERATION FOR CONDUCTION LOSSES

In the unipolar switching method, the turn-on period of low side switches is one and half times longer than the turn-on Period of high-side switches.

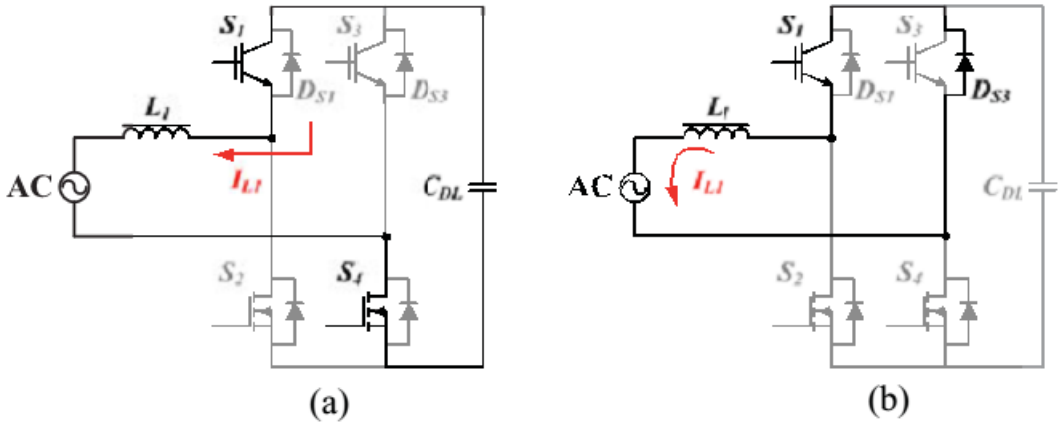

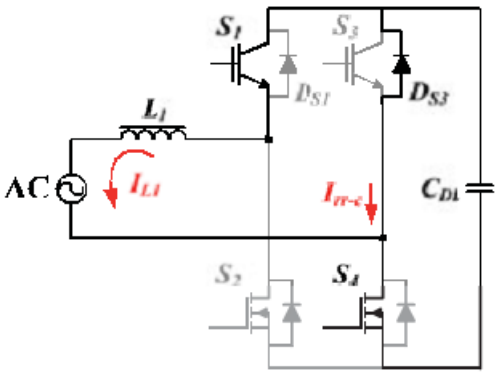

(e)

Fig 4 Operating modes in the rectifier's generation mode using the inverted switching pattern against the rectification mode: (a) Mode1, (b) Mode2, (c) Mode3, (d) Mode4 and (e) Mode5.

To analyse the conduction loss of MOSFETs as the low-side switches, the circuit operation of the proposed bidirectional rectifier assumes that inductor L1 is sufficiently large to operate CCM and the ac input current is a perfectly sinusoidal waveform. Generally, the conduction loss in MOSFETs can be calculated using the rms current passing through MOSFET's $R_{DS\cdot on.}$ Since the turn-on period of the low-side switches is 75% of the fundamental period of the ac input current, the rms current of the low side switches can be calculated using the following equation:

$$I_{\text{rms.low}} = \sqrt{\frac{1}{2\pi}\int_{o}^{\frac{3}{2}\pi} (I_{\text{in}.P}\sin\omega t)^2 d\omega t.} \tag{1}$$

Through the aforementioned assumptions, the peak current $I_{in.p}$ and the average current $I_{in.av}$ of the ac input can be derived as follows:

$$I_{\text{in}.P} = \sqrt{2}\frac{P_{\text{out}}}{\eta V_{\text{in.rms}}} \tag{2}$$

$$I_{\text{in.av}} = \frac{2}{\pi} I_{\text{in}.P} \tag{3}$$

Where η is the power conversion efficiency. Using the aforementioned equations, the total conduction losses of the rectifier's switches in the rectification can be calculated as follows:

$$P_{\text{con-rec}} \simeq 2(I_{\text{rms.low}})^2 R_{\text{DS.on}} + 2\left(\frac{1}{4} I_{\text{in.av}}\right) V_F$$

$$= \frac{3}{4} I_{\text{in}.P}^2 R_{\text{DS.on}} + \frac{1}{\pi} I_{\text{in}.P} V_F \tag{4}$$

Where the conduction loss in the rectification mode is Pcon-rec and VF is the forward voltage drop of the high-side SiC diode, respectively. In comparison to using IGBTs for the low-side switches. The low-side switches use MOSFETs, which have extremely low $R_{DS.on}$ and the latest IGBTs, which have the very low collector– emitter threshold voltage VCE. The high side switches use SiC diodes as the antiparallel diode and IGBTs without anti parallel diode. The typical values of $R_{DS.on}$, VF, and VCE are obtained from their datasheets. Since VF and VCE are almost the same value, the conduction loss in the generation mode is expected to be nearly the same as the conduction loss in the rectification mod, $P_{con\text{-}rec}$. Under the light-load condition, MOSFETs is better than IGBTs in the view point of the power conversion efficiency. At the rated load (5 kW), the difference of the conduction losses between MOSFETs and IGBTs is about 12 W. If two MOSFETs are used in parallel, the conduction losses in the rated load will be reduced about 30 W.

D. SRF-PLL WITH ENHANCED FREQUENCY ESTIMATOR

For the application of the grid-interactive power converters, the phase estimation of the supply voltage is required to control the entire power system; especially, the phase information of the supply voltage is mandatory to generate the current reference. The phase estimation method requires robustness to noise and disturbance from grid, accuracy to the fundamental frequency variation and harmonic distortion, and easy implementation using analog or digital platforms. The SRF-PLL is one of the popular methods. It has a weak point of a frequency tracking performance. In Fig 5, the constant angular frequency of the fundamental component ωs is used as a feed forward term for compensating the phase angle tracking. It can cause a tracking error in the PLL operation when the fundamental frequency changes to the different value of the constant ωs.

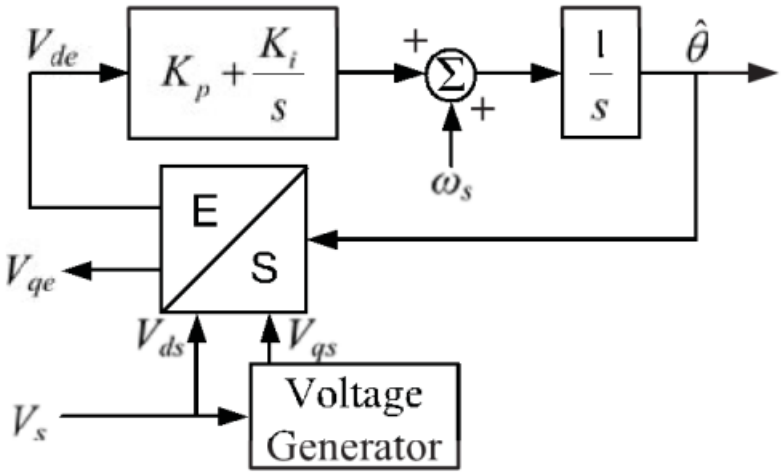

Fig 5 Block diagram of a conventional single-phase SRF-PLL.

To track unexpected fundamental frequencies, the SRF-PLL requires a frequency estimator instead of the constant angular frequency. The SRF-PLL method uses the π/2 phase-shifted wave of the supply voltage using the all-pass filter (APF). Therefore, the PLL has four zero crossing points in a period of the supply voltage and they are located at every π/2. It means that the frequency information can be obtained at every quarter of the period. However, the conventional research has updated the frequency information at every half of the period. Consequently, the proposed frequency detection algorithm illustrated in Fig 6(a) can update the variation of the supply frequency two times faster than the conventional one. In the algorithm, there are two time zones to calculate the supply period: Tc and Td where Tc is the time duration between two zero crossing points and Td is the time duration near the zero crossing point. Td is introduced to implement a practical PLL system using the proposed algorithm since noises in the power stage and sensors make the exact detection of the zero crossing points imperfect. In Fig 6 (a), the supply frequency can be estimated as shown in

$$\hat{f}_s = \frac{1}{4(T_c + T_d)}. \tag{5}$$

The FIR low-pass filter (LPF) illustrated in Fig 6 (b) is adapted to the proposed frequency detector instead of a moving average (MA). The filtered output can be calculated as follows:

$$s_f[n] = \sum_{k=0}^{7} b_k s[n-k] \tag{6}$$

Where s[n] is the nth input signal, sf[n] is the nth filtered signal, and bk is the kth-order filter coefficient. This filter has seventh order and uses the Blackman window to enhance the sharpness of the filter at the cut-off frequency and to suppress side lobe components. It can improve the transient dynamics and reduce the steady-state error of the frequency detector.

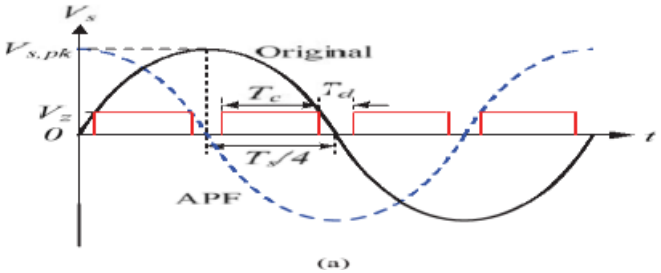

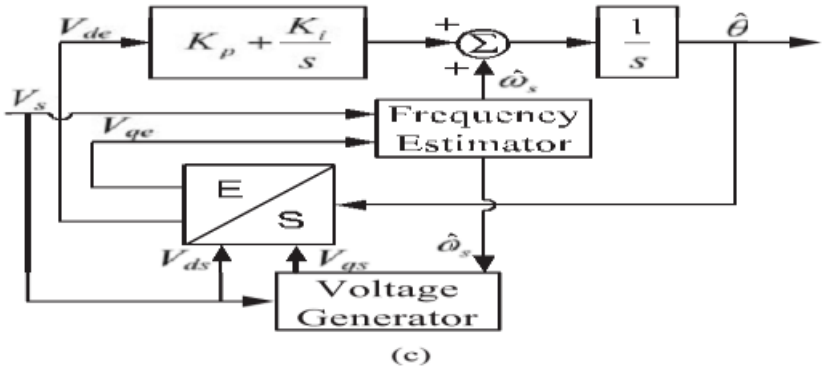

Fig 6 Proposed single-phase PLL method: (a) frequency detection algorithm using zero crossing and APF, (b) block diagram of the seventh-order FIR filter, and (c) block diagram of the PLL using the proposed frequency estimator

The simulation result of the HD with MA, which is the conventional one, shows high fluctuation and long settling time in the fundamental frequency detection. However, the simulation result of QD with MA shows low fluctuation and short settling time because of the shorter update duration than the case of HD. In addition, QD with FIR filter has higher transient dynamics and faster convergence than the case of QD with MA because of the seventh-order FIR filter using the Blackman window instead of MA.

IV.ISOLATED BIDIRECTIONAL CLLC RESONANT CONVERTER

In this section, the design methodology of the power stages of the proposed bidirectional CLLC resonant converter will be discussed. The new control schemes are proposed to decide power flow directions and to regulate output voltage under bidirectional power flows. In addition, the dead-band control algorithm is proposed to smoothly change the power conversion direction only using output voltage information. This algorithm is based on a hysteresis control method to -decide the power flow direction of bidirectional converters.

A.GAIN ANALYSIS USING THE FHA MODEL

The first harmonic approximation (FHA) model and operation mode in the proposed CLLC resonant converter are already introduced in [18]. Fig 7 shows the equivalent circuit of the proposed full-bridge bidirectional CLLC resonant converter using the FHA method. The resonant network of the converter is composed of the series resonant capacitor Cr =Cr1 =Cr2, the equivalent series resonant inductance Leq, and the magnetizing inductance Lm. Since the turn ratio of the transformer is 1:1, it does not affect the circuit model and Leq equals the twice of the series resonant inductance Lr =Lr1 =Lr2. The forward transfer function Hr of the resonant network can be derived as shown in

$$H_r(s) = \frac{V_{o,\mathrm{FHA}}(s)}{V_{i,\mathrm{FHA}}(s)} = \frac{Z_o(s)}{Z_{\mathrm{in}}(s)} \cdot \frac{R_{o,e}}{(sC_r)^{-1} + R_{o,e}} \tag{7}$$

$$Z_{\mathrm{in}}(s) = \frac{1}{sC_r} + sL_{\mathrm{eq}}(s) + Z_o(s) \tag{8}$$

$$L_{\mathrm{eq}}(s) = \frac{L_r}{s^2 L_m L_r [R_o(sL_m + sL_r + R_o)]^{-1} + 1} \tag{9}$$

$$Z_o(s) = \frac{L_m C_r^{-1} + sL_m R_{o,e}}{sL_m + (sC_r)^{-1} + R_{o,e}}, R_{o,e} = \frac{8}{\pi^2} R_o. \tag{10}$$

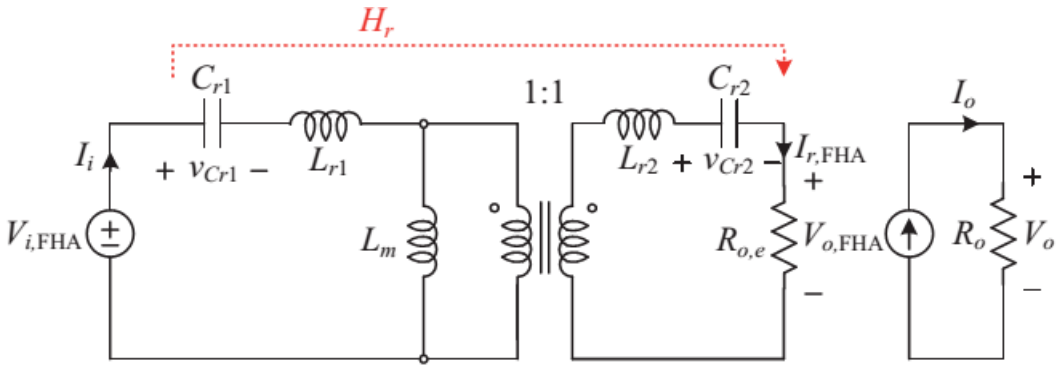

Fig 7 FHA model of the proposed bidirectional CLLC resonant converter

Therefore, the gain of converter //Hr// can be derived as follows:

$$\frac{V_o}{V_{\text{in}}} = \|H_r(f_n)\| = \frac{f_n^3}{\sqrt{f_n^2 A^2(f_n) + Q^2 B^2(f_n)}} \tag{11}$$

Where A(fn) and B(fn) are the function components as follows:

$$A(f_n) = -f_n^2(1+k) + k \tag{12}$$

$$B(f_n) = f_n^4 - f_n^2(2+k) + k. \tag{13}$$

In addition, fn can be described using the resonant frequency fr, Q is the quality factor, and k is the inductance ratio between the magnetizing and leakage inductance, respectively, given by

$$f_n = \frac{f_s}{f_r}, f_r = \frac{1}{2\pi\sqrt{L_r C_r}}, Q = \frac{Z_r}{R_{o.e}}, Z_r = \sqrt{\frac{L_r}{C_r}}, k = \frac{L_r}{L_m}. \tag{14}$$

The gain has a peak value at low resonant frequency which contains the magnetizing inductance as a resonant component. At high resonant frequency, the gain of the converter is slightly higher than unity gain. Under the light-load condition, the gain is high and the slope of the gain curve is sharp. However, the overall value of the gain curve is decreasing under the heavy-load condition. The higher load induces the lower gain in the proposed bidirectional CLLC resonant converter.

B.SOFT-SWITCHING CONDITIONS

The ZVS operation of the primary power MOSFETs and the soft commutation of the output rectifiers are significant factors for the efficiency-optimal design of the bidirectional full-bridge CLLC resonant converter. The lower operating frequency than the resonant frequency can guarantee the soft commutation of the output rectifiers because the difference between the switching frequency and the resonant frequency makes discontinuous rectifying current. In addition, during the dead time of the switches, the primary current should discharge the output capacitance of four primary switches for their ZVS turn-on. Therefore, the magnetizing inductance is limited by the maximum operating frequency as shown in

$$f_s \le f_r \tag{15}$$

$$L_m \le \frac{t_{dt}}{16 C_S f_{s,\max}} = \frac{t_{dt}}{16 C_S f_r}. \tag{16}$$

Inequality (16) shows that small Lm can guarantee the ZVS of main switches. However, small Lm also increases the conduction loss of MOSFETs, transformer windings, and output rectifiers in the primary and secondary sides. On the other hand, the large magnetizing inductance satisfied with (15) can reduce the conduction loss and improve the power conversion efficiency of the converter. However, large Lm can make a gain reduction below the unity gain in the proposed bidirectional CLLC resonant converter.

C. DEAD-BAND CONTROL FOR BIDIRECTIONAL OPERATION

Fig 8 (a) shows the theoretical waveforms of the proposed dead-band control algorithm for the bidirectional CLLC resonant converter When the load becomes negative, the output voltage of the converter will drastically increase because power is supplied to the output capacitor from two sides: the converter side and the load side. At this time, the converter is uncontrollable without changing the power conversion mode because of the negative power flow. If the output voltage reaches the positive dead-band voltage +Vb and, the power conversion mode changes from the powering mode to the generating mode. In this generating mode, the converter transfers power from load to input side. Then, the output voltage will decrease to the reference voltage Vref, which will be regulated by a pulse frequency modulation (PFM) controller. In the same manner, the power conversion mode can be changed from the generating mode to the powering mode. This dead band controller generates the sign of the voltage error Verr which is the voltage difference between the output voltage and the reference voltage. The PI controller regulates the output voltage using Verr and its sign. The switch control block generates PFM switching pulses using the calculated switching frequency generated by the PI controller. Finally, the PFM switching pulses are assigned to the proper power switches considering the power conversion mode.

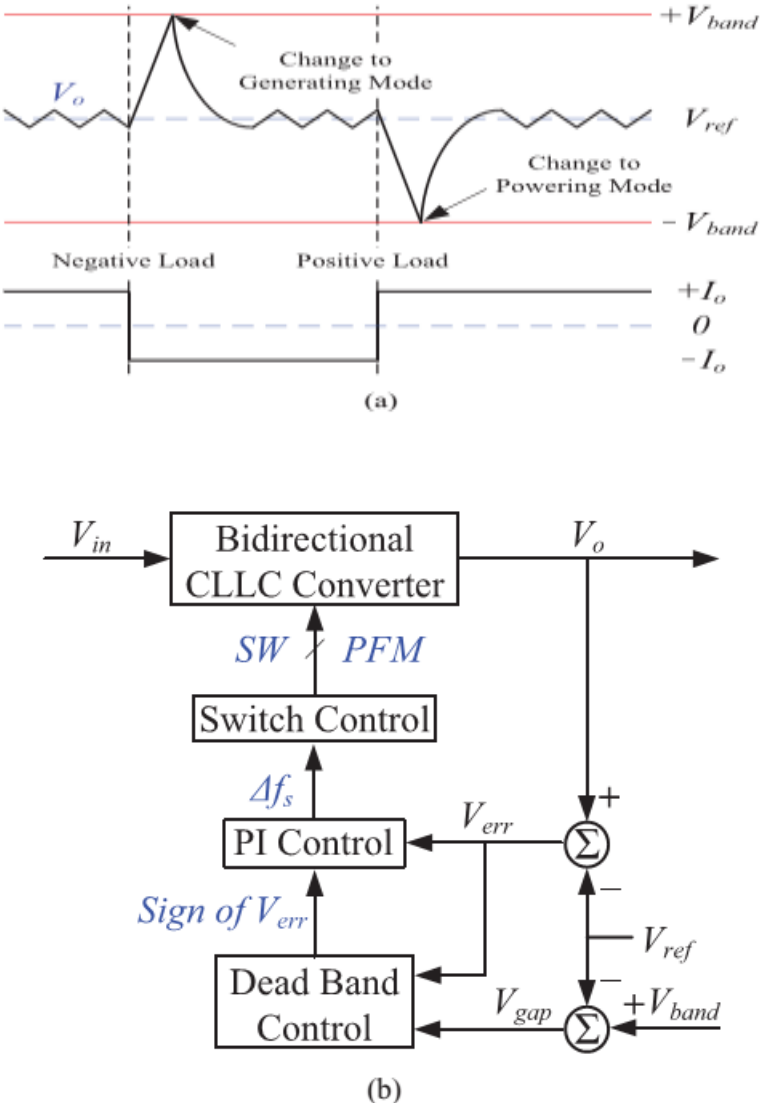

Fig 8 Schematics of the proposed dead-band control algorithm: (a) theoretical waveforms and (b) block diagram of the control algorithm

V.MATLAB/SIMULINK RESULTS

Here the simulation is carried out by two different cases 1) proposed isolated bidirectional ac–dc converter 2) proposed converter with of DC machine as load

Case-1 proposed isolated bidirectional ac–dc converter

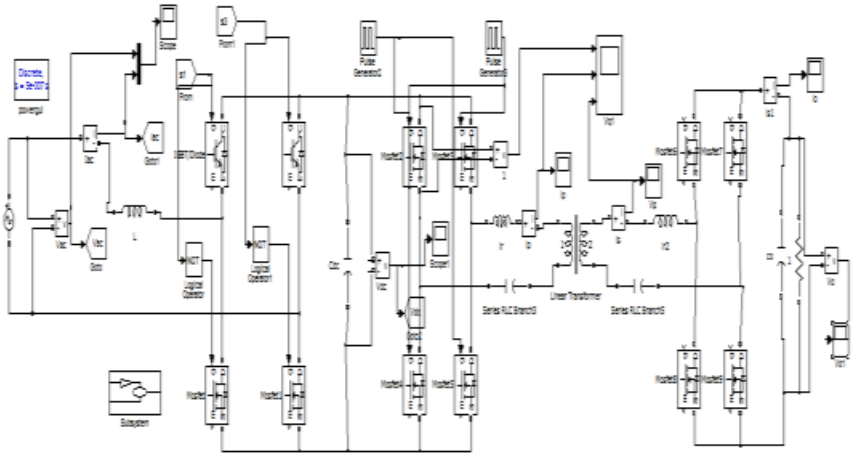

Fig.9 MATLAB/simulink model of isolated bidirectional ac–dc converter

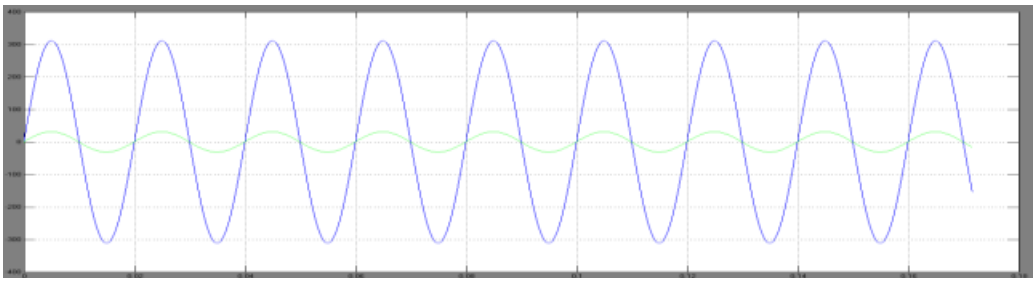

(a)

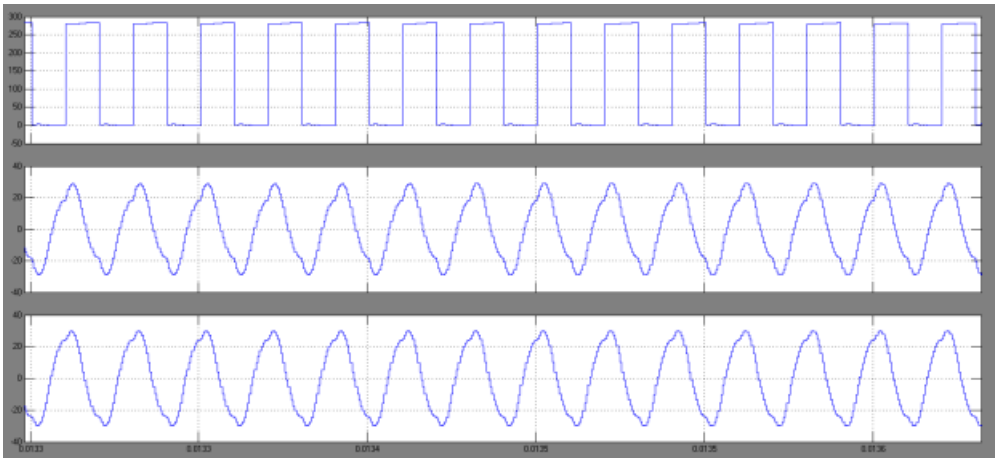

(b)

Fig. 10 (a) input voltage and current with dc-link voltage in the ac– dc rectifier and (b) resonant currents with output voltage in the dc– dc converter

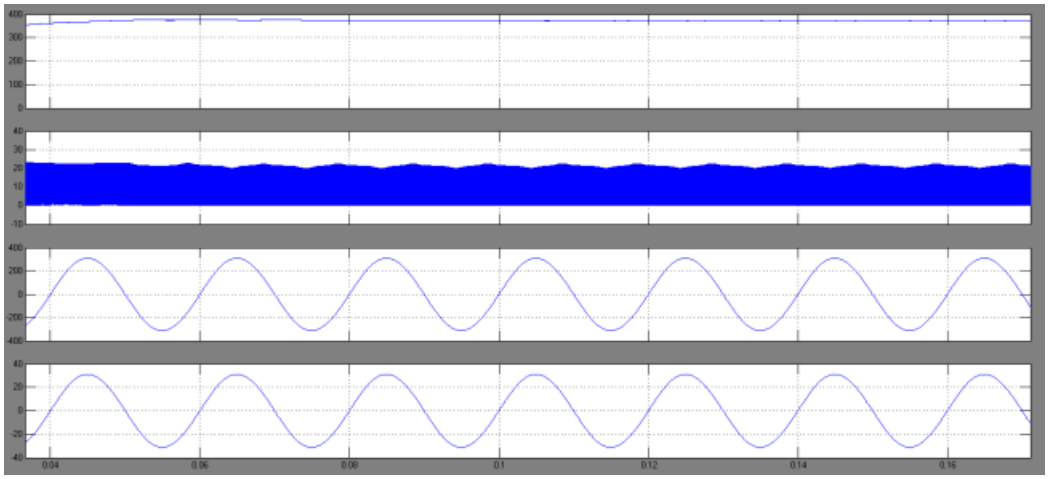

(a)

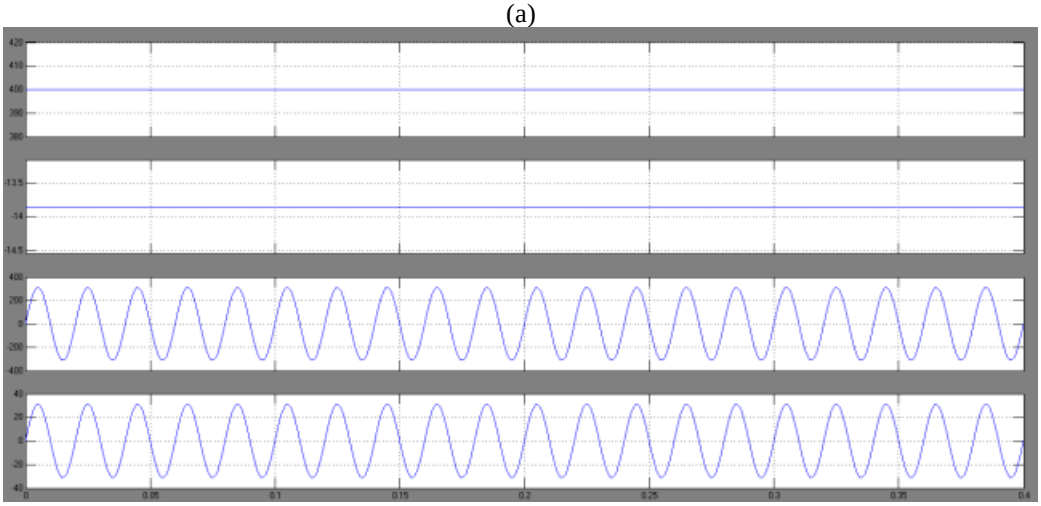

(b)

Fig.11 output waveforms of the bidirectional operation at full load: (a) rectification mode and (b) generation mode

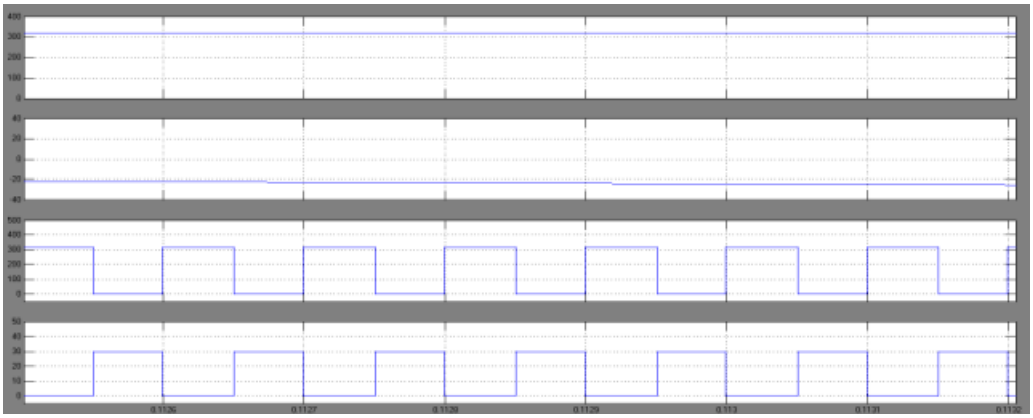

(a)

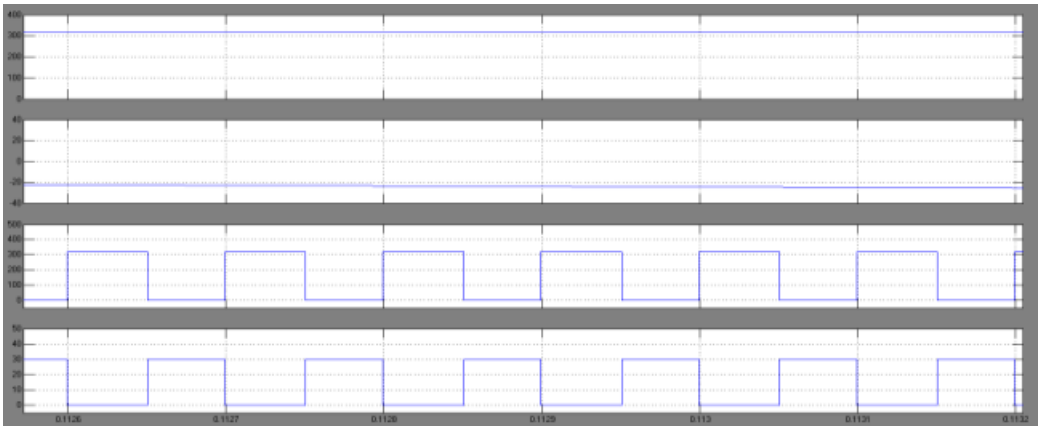

(b)

Fig. 12 Switching waveforms of the ac–dc rectifier using FRD and SiC diode (a) FRD case and (b) SiC diode case

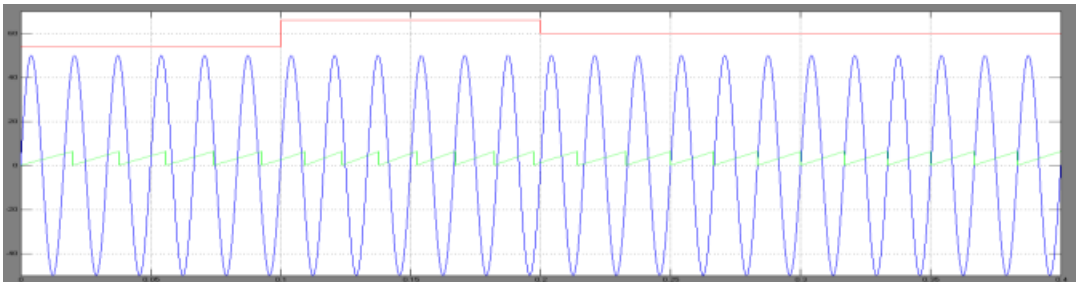

Fig.13.simulation results of phase detection performance conventional SRF-PLL and

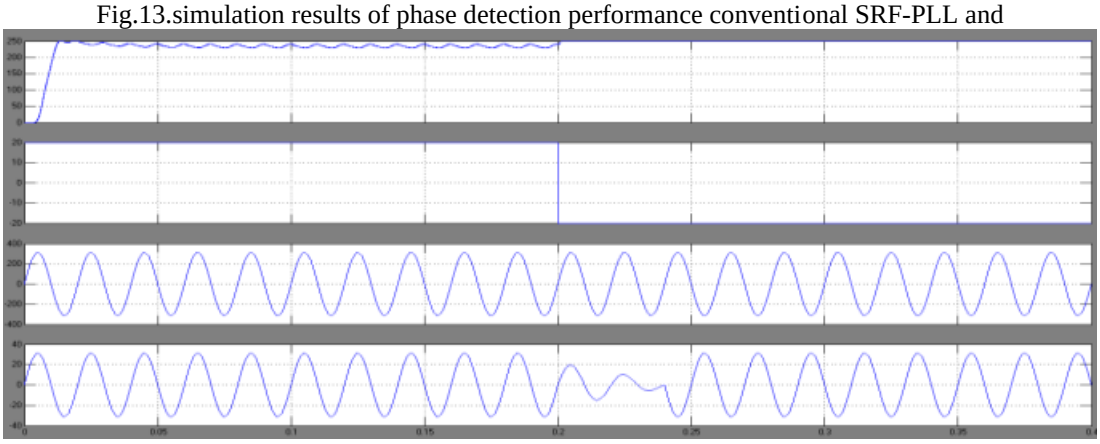

Fig.14 Step load response of overall bidirectional converter ac–dc rectifier part.

Case-2 proposed converter with DC drive

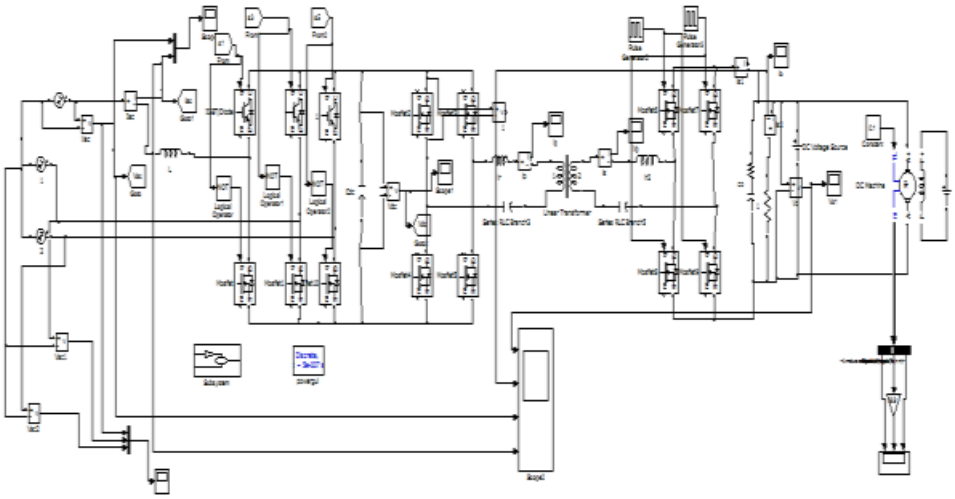

Fig.15 MATLAB/simulink model of proposed converter with of DC machine

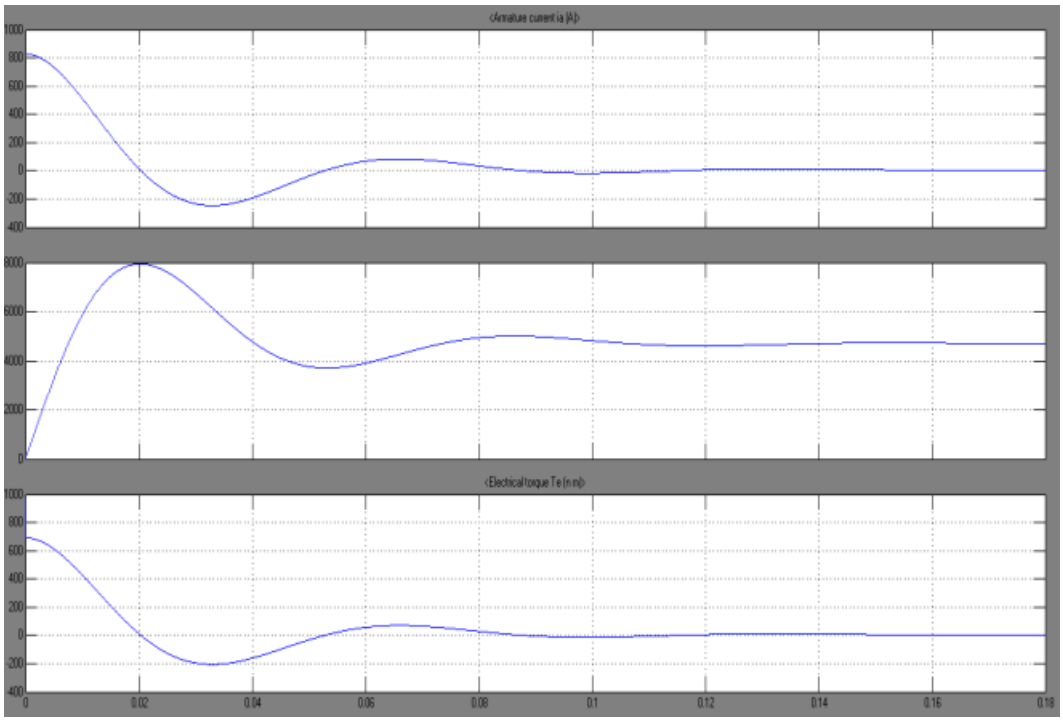

Fig.16 shows the output waveforms of stator current, speed and electromagnetic torque of DC machine

VI.CONCLUSION

In this paper the proposed isolated bidirectional ac– dc converter is connected to of DC machine as load and to check the performance of speed and torque. The isolated bidirectional ac–dc converter is proposed for the 380-V dc power distribution system to control the bidirectional power flow and to improve its power conversion efficiency. In order to improve the reverse recovery problem, the high-side switches of the ac– dc rectifier employ IGBTs without ant parallel diodes and SiC diodes. In addition, the low-side switches are composed of two MOSFETs to reduce the conduction loss in the rectification mode. For comparison with the conventional IGBT switches, the total conduction losses of the rectifier's switches are calculated in the rectification mode. The simple and intuitive frequency detection method for the single-phase SRF-PLL is also proposed using the filter compensator, fast QD, and FIR filter to improve the robustness and accuracy of the PLL performance under fundamental frequency variations. The proposed PLL system shows lower detection fluctuation and faster transient response than the conventional techniques. Finally proposed converter results are verified through MATLAB /Simulink software.

REFERENCES

[1] G.-S. Seo, J. Baek, K. Choi, H. Bae, and B. Cho, "Modeling and analysis of dc distribution systems," inProc. IEEE 8th Int. Conf. Power Electron. ECCE Asia, May 2011, pp. 223–227.
[2] K. Techakittiroj and V. Wongpaibool, "Co-existance between a distribution and dc-distribution: In the view of appliances," in Proc. 2nd Int. Conf. Comput. Electrical Eng., Dec. 2009, vol. 1, pp. 421–425.
[3] A. Stupar, T. Friedli, J. Minibock, and J. Kolar, "Towards a 99% efficient three-phase buck-type PFC rectifier for 400-V dc distribution systems," IEEE Trans. Power Electron., vol. 27, no. 4, pp. 1732–1744, Apr. 2012.
[4] T.-F. Wu, C.-L. Kuo, K.-H. Sun, and Y.-C. Chang, "DC-bus voltage regulation and power compensation with bi-directional inverter in dc-micro grid applications," in Proc. IEEE Energy Convers. Congr. Expo., Sep. 2011, pp. 4161–4168.
[5] B.-R. Lin and Z.-L. Hung, "A single-phase bidirectional rectifier with power factor correction," inProc. IEEE Energy Convers. Congr. Expo. Aug. 2001, vol. 2, pp. 601–605.
[6] Y. Zhangang, C. Yanbo, and W. Chengshan, "Construction, operation and control of a laboratory-scale micro grid," in Proc. Int. Conf. Sustainable Power Generation Supply, Apr. 2009, pp. 1–5.
[7] W. Ryckaert, K. De Gusseme, D. Van de Sype, L. Vandevelde, and J. Melkebeek, "Damping potential of single-phase bidirectional rectifiers with resistive harmonic behaviour,"IEE Electric Power Appl., vol. 153, no. 1, pp. 68–74, Jan. 2006.
[8] T.-F. Wu, K.-H. Sun, C.-L. Kuo and C.-H. Chang, "Predictive current controlled 5-kW single-phase bidirectional inverter with wide inductance variation for dc-micro grid applications," IEEE Trans. Power Electron., vol. 25, no. 12, pp. 3076–3084, Dec. 2010.
[9] D. Dong, F. Luo, D. Boroyevich, and P. Mattavelli, "Leakage current reduction in a single-phase bidirectional ac-dc full-bridge inverter," IEEE Trans. Power Electron., vol. 27, no. 10, pp. 4281– 4291, Oct. 2012.
[10] K. H. Edelmoser and F. A. Himmelstoss, "Bidirectional dc-to dc converter for solar battery backup applications," in Proc. IEEE 35th Annu. Power Electron. Spec. Conf., Jun. 2004, vol. 3, pp. 2070–2074.
[11] D. Salomon son, L. Soder, and A. Sannino, "Protection of low-voltage dc micro grids,"IEEE Trans. Power Del., vol. 24, no. 3, pp. 1045–1053, July 2009.